

Optical, magneto-optical, and magnetic properties of stoichiometric and off-stoichiometric γ' -phase Ni_3Al alloys

Joo Yull Rhee*

Department of Physics, Hoseo University, Asan, Choongnam 336-795, Korea

Y. V. Kudryavtsev

Institute of Metal Physics, NASU, 36 Vernadsky str, 252680, Kiev-142, Ukraine

Y. P. Lee[†]

Quantum Photonic Science Research Center and Department of Physics, Hanyang University, Seoul 133-791, Korea

(Received 1 January 2002; revised 10 February 2003; published 1 July 2003)

The optical and magneto-optical properties of two γ' -phase Ni_3Al alloys ($\text{Ni}_{0.752}\text{Al}_{0.248}$ and $\text{Ni}_{0.771}\text{Al}_{0.229}$) have been investigated experimentally and theoretically. In the optical-conductivity spectra of the investigated alloys two intense interband absorption features at ~ 0.8 eV and ~ 4.2 eV were experimentally observed. The peak at ~ 0.8 eV was theoretically predicted, but not experimentally confirmed in the previous investigations. The low-energy peak exhibits a multiple-peak structure for $\text{Ni}_{0.771}\text{Al}_{0.229}$ alloy. It is also theoretically shown that the fine structure of the low-energy absorption features originates from the extra spin ordering due to the appearance of the so-called antistructure Ni atoms and their clusters in the $\text{Ni}_{0.771}\text{Al}_{0.229}$ alloy, and it is experimentally shown that this fine structure persists up to room temperature. The temperature dependencies of the optical and magneto-optical properties of $\text{Ni}_{0.771}\text{Al}_{0.229}$ alloy can be ascribed to the presence of magnetic inhomogeneity in the sample. The existence of magnetic inhomogeneity in the alloy is further confirmed by the ac magnetic-susceptibility measurements in which the susceptibility curve exhibits two magnetic transitions, one at 87.5 K and the other at 252 K. The spin ordering (paramagnetic-to-ferromagnetic transition) and Ni enrichment play a key role for the physical properties.

DOI: 10.1103/PhysRevB.68.045104

PACS number(s): 78.20.Bh, 75.10.Lp, 71.15.Mb

I. INTRODUCTION

The intermetallic compound Ni_3Al has received considerable attention over the last several decades because of its peculiar physical properties. Among its various physical properties the optical property is controversial. The measured results of the dielectric function of the Ni_3Al alloy have been reported only twice.^{1,2} van der Heide *et al.*¹ measured the dielectric function by spectroscopic ellipsometry in the 0.5–5.3-eV region. The optical-conductivity (OC) spectrum showed a weak shoulder at 0.86 eV and a broad but pronounced peak at 4.32 eV. Rhee *et al.*² also measured the dielectric function by spectroscopic ellipsometry in the 1.5–5.3-eV region. The shape of the measured OC spectrum in the high-energy side was similar to that of Ref. 1, while the magnitude was almost 50% larger. Rhee *et al.*² attributed the discrepancy to the different preparation method of the sample surface.

In Ref. 1 it was claimed that the experimental results were in good agreement with the theoretical calculations using the band structure of Ref. 3. However, it should be noted that in their calculations the dipole-transition-matrix elements were not included. In addition, as it was shown later, the inclusion of the dipole-transition-matrix elements leads to drastic changes in the shape of the calculated OC spectra, especially in the low-energy region. According to the results of the latter calculations an intense interband absorption peak near 1 eV should be observed in the OC spectrum for the Ni_3Al alloy.^{2,4} The controversy between the prediction of theory and the existing experimental results needs to be resolved.

Therefore, an additional experimental study of the optical properties of two (stoichiometric and off-stoichiometric) γ' -phase Ni_3Al alloys, mainly in the near-infrared (NIR) region of the spectrum, is desirable.

We indeed observed strong interband absorption features in the NIR region. Additionally, in the course of investigation the temperature dependence of the OC spectra was measured. These measurements revealed that the multiple-peak structure had strong temperature dependence, and, especially, that a double-peak structure centered at 0.8 eV persisted up to room temperature (RT).

It is well known that the optical as well as the magneto-optical (MO) properties of metals and alloys are closely related to their electronic band structure. According to Pells and Shiga,⁵ for instance, fine structures of the main absorption peak in the OC spectrum of pure Ni originates from the overlapping of two peaks contributed by the electronic excitations from both minority- and majority-spin subbands separated by the exchange splitting. This study of the temperature dependence of the OC spectrum for Ni allowed the authors to make a conclusion regarding the temperature behavior of the energy-band structure of pure Ni.

Based on this discussion we can argue that our observations, particularly those of the temperature dependence, are quite possibly related to the peculiar magnetic properties of the alloys. Therefore, we investigated two more physical properties: the MO and magnetic properties.

The MO tools in some sense combine the advantages of both optical and magnetic approaches. Therefore, it can be expected that the study of the MO and optical properties of

the γ' -phase Ni_3Al alloys will also be useful for understanding the peculiarities of their magnetic properties. As far as we know, the MO properties of the Ni_3Al alloys have not yet been investigated.

It is generally believed that the γ' -phase Ni_3Al alloy has an itinerant-type weak ferromagnetism. Several investigations of the magnetic properties were conducted to clarify the origin of the magnetism,^{6–12} however, it is still a matter of controversy. The Curie temperature, T_C , of the alloy, at which the average magnetization vanishes, strongly depends on the Ni concentration.^{6–11} In addition, even for the same stoichiometry, different groups reported different values of T_C . For a sample with 75 at. % of Ni concentration, T_C varies from 40.6 K (Ref. 10) to 43.5 K,¹¹ and Semwal and Kaul¹² even claimed that they obtained a much higher Curie temperature, $T_C=56.46$ K. On the other hand, the reported magnetic moment for the Ni atom is about $0.075\mu_B$ and it is well confirmed.^{6,7,10–12} There is one exception: in Ref. 9 it is $0.077\mu_B/\text{atom}$, equivalent to $0.103\mu_B/\text{Ni atom}$.

The explanation for the origin of magnetic behavior of the alloy is even more variant. Three different scenarios were proposed: (i) the Stoner-Edwards-Wohlfarth model,¹³ (ii) the self-consistent renormalization of the spin-fluctuation model,¹⁴ and (iii) a modified self-consistent renormalization¹² of the spin-fluctuation model utilizing the Ginzburg-Landau formalism.¹⁵ There was evidence for well-defined spin-wave excitations, obtained by small-angle neutron scattering¹⁶ and inelastic neutron-scattering¹⁷ experiments. Dhar *et al.*¹⁸ found an upturn by the influence of magnetic fields in the low-temperature region of the C/T -vs- T^2 plot and attributed it to an enhancement of the effective electronic mass due to the spin fluctuations. They also found a crossover at a Ni concentration of 75.1 at. % from a spin fluctuator to a ferromagnet as the Ni concentration increases. The possibility of the presence of superparamagnetic clusters^{19–21} or, at least, a magnetic inhomogeneity⁷ in the sample was suggested, while there were also opposing opinions.^{22,23}

Because of the aforementioned dispute, several theoretical investigations using the electronic-energy-band-structure calculations were followed in order to elucidate the origin of weakly itinerant ferromagnetism of the alloy.^{3,24,25} Hackenbracht and Kübler²⁴ employed the linear-muffin-tin-orbital (LMTO) method using the atomic-sphere approximation (ASA) and found that the magnetic moment was $0.031\mu_B/\text{Ni atom}$ which is only 40% of the experimental value.^{6,7,10–12} Later Buiting *et al.*³ argued that Ni_3Al is still in the fluctuation regime even though it is in a ferromagnetic state. The calculated magnetic moment almost vanished at the experimental lattice constant ($a=3.568$ Å), while it was calculated to be $0.067\mu_B/\text{Ni atom}$, which is close to the experimental value, at a lattice constant of 3.583 Å. Min *et al.*²⁵ also investigated the electronic structures and magnetic properties of Ni_3Al . The calculated magnetic moment was $0.15\mu_B/\text{Ni atom}$ and the authors argued that the spin-orbit interaction might reduce the calculated magnetic moment to $0.087\mu_B/\text{Ni atom}$, since the spin-orbit interaction would reduce the exchange splitting by $\sim 40\%$.

It can be assumed that the disagreement among various experimental data as well as between the experimental and theoretical results can be ascribed to the deviation of the actual alloy composition from the nominal one and/or some disorderedness of the experimentally investigated alloys.¹⁸ Therefore, it seems desirable to carry out a theoretical study of the influence of the atomic disorder and/or deviation from the stoichiometric composition on the magnetic properties of γ' -phase Ni_3Al alloys.

In this paper we report the results of theoretical and experimental studies of the optical, MO, and magnetic properties of the stoichiometric and slightly off-stoichiometric γ' -phase Ni_3Al alloys. The intense peak near 1 eV predicted by theory is experimentally confirmed. The peak is not only very strong but there are actually also multiple peaks in the ferromagnetic state. The multiple-peak structure is very sensitive to temperature and persists up to RT. The MO response also persists up to RT. We interpret these observations to be a result of the presence of magnetic inhomogeneities and/or clusters in the investigated alloys.

II. EXPERIMENTAL PROCEDURES

For the experimental part of the study two bulk samples, $\text{Ni}_{0.752}\text{Al}_{0.248}$ and $\text{Ni}_{0.771}\text{Al}_{0.229}$, were prepared. The alloy composition was checked with an x-ray fluorescence technique. We hereafter refer to these two alloys as STOICH ($\text{Ni}_{0.752}\text{Al}_{0.248}$) and OFF-STOICH ($\text{Ni}_{0.771}\text{Al}_{0.229}$) alloys. The structural homogeneity of samples was studied using x-ray diffraction (XRD). The magnetic properties of the alloys in the 4.2–300-K temperature range were investigated by measuring the ac magnetic susceptibility.

The descriptions of sample preparation and surface treatment for the optical measurements are given elsewhere.²⁶ The optical properties of the STOICH alloy were also measured at RT, while those of the OFF-STOICH alloy were investigated at several temperatures, i.e., at 20, 90, 293, 380, and 480 K. The spectral dependence of the MO equatorial Kerr effect (EKE) of the OFF-STOICH alloy was measured in the ferromagnetic state at 27 K by the dynamical method using the p -plane-polarized light at an angle of incidence of 77° in a spectral range of 0.6–4.0 eV and in an ac magnetic field of 3 kOe. The EKE value, $\delta_p = \Delta I/I_o$, is the relative change in the intensity of the reflected light, caused by the magnetization of sample in an external magnetic field directed transversely to the plane of incidence. The temperature dependence of the EKE value was measured at a fixed photon energy ($\hbar\omega=4.0$ eV) in a temperature range of 20–320 K at an angle of incidence of 70° .

III. THEORETICAL CALCULATIONS

In order to determine the origin and, especially, the temperature dependence of the low-energy multiple-peak features, we performed electronic-structure calculations for the $L1_2$ structure of the stoichiometric alloy and two different types of supercell calculations for slightly “disordered” and Ni-rich alloys to calculate the OC spectra with the dipole-transition-matrix elements. The OC spectra were obtained for

both paramagnetic and ferromagnetic phases of the perfectly ordered, stoichiometric Ni_3Al alloy and for a slightly Ni-rich $\text{Ni}_{25}\text{Al}_7$ alloy which is equivalent to the $\text{Ni}_{0.78125}\text{Al}_{0.21875}$ alloy composition. These calculational results can be used for understanding the experimentally observed¹³ strong concentration dependence of the magnetization, $M \propto (x - x_c)^{1/2}$, where M is the magnetization at $T=0$ K and $x_c (=0.745)$ is the critical concentration above which the sample becomes ferromagnetic, and it is also the magnetic inhomogeneity. We employed the scalar-relativistic version of the tight-binding LMTO-ASA method²⁷ within the local-density approximation²⁸ and the local-spin-density approximation²⁹ (LSDA) for the paramagnetic and the ferromagnetic phases, respectively. The spin-orbit interactions were included in a perturbative way. The experimental lattice constant of 3.568 Å was used, and the atomic-sphere radii were 1.439 Å and 1.380 Å for Al and Ni, respectively. The band structures and the densities of states of the stoichiometric alloy in the paramagnetic phase are in a close agreement with those obtained in previous calculations.^{2,3,24,25}

For the first type of supercell calculations, we kept the stoichiometry of the Ni_3Al alloy and simply interchanged the Ni and Al atoms in certain Ni-Al atom pairs to simulate some “disorder.” To do this we expanded the unit cell to a $2 \times 2 \times 2$ supercell which contains eight simple-cubic $L1_2$ unit cells. There are two choices of the interchange between Ni and Al atoms: interchange between the nearest neighbors, i.e., Al(0,0,0) and Ni($\frac{1}{4}, \frac{1}{4}, 0$) (disorder I), and interchange between the third-nearest neighbors, i.e., Al(0,0,0) and Ni($\frac{1}{2}, \frac{1}{4}, \frac{1}{4}$) (disorder II). The former does not allow to form complete nine-atom Ni clusters, while the latter does. The calculational results show a certain reduction in the magnetic moments of the slightly “disordered” samples compared to the perfectly ordered one.

The second type of supercell calculations used a defect-specified supercell technique.³⁰ We used the same $2 \times 2 \times 2$ supercell as employed for the above “disordered” samples. We only substituted an Al atom at the origin by a Ni atom and, therefore, the stoichiometry of the sample used in this defect-specified supercell calculation is $\text{Ni}_{25}\text{Al}_7$ (or $\text{Ni}_{0.78125}\text{Al}_{0.21875}$).

IV. RESULTS AND DISCUSSION

The structural homogeneity of the investigated samples seemed to be a single phase. Only diffraction lines related to the γ' phase can be observed on the XRD spectrum for the Ni-rich Ni_3Al alloy (see Fig. 1). The amount of second phase, if any, should be too small to be detected by XRD or have an indistinguishable crystal structure from the dominant phase (see below).

The measured OC spectrum at 293 K for the STOICH alloy together with the results of theoretical calculations are shown in Fig. 2. Figure 3(a) presents the experimental OC spectra at several temperatures for the OFF-STOICH alloy. The overall shape of spectra and the position of a broad high-energy peak of the experimentally obtained OC spectra at 293 K for the investigated alloys are in an excellent agreement with the

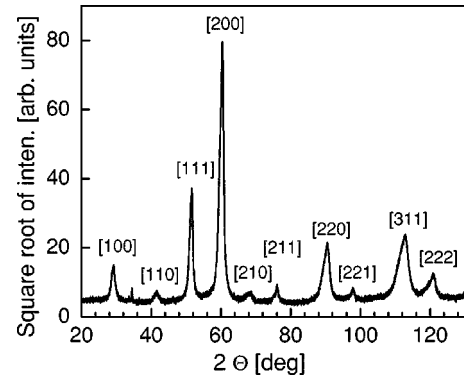


FIG. 1. X-ray-diffraction spectrum for the off-stoichiometric $\text{Ni}_{0.771}\text{Al}_{0.229}$ alloy taken at Co $K\alpha$ radiation.

previous measurements.^{1,2} The magnitude of OC for the OFF-STOICH alloy is similar to that in Ref. 1, but smaller than that in Ref. 2, while for the stoichiometric composition the magnitude of OC in the ultraviolet (UV) region is nearly the same as that in Ref. 2. The magnitude of OC is sensitive to the surface conditions and treatments,³¹ while the energy locations of structures in the spectrum are not. Some discrepancy in the magnitude of these experimental OC spectra can be related to the differences in sample preparation.

The main difference between the present measurements for both alloys and the previous ones^{1,2} is an intense absorption peak around 0.8 eV for the STOICH alloy. This peak was

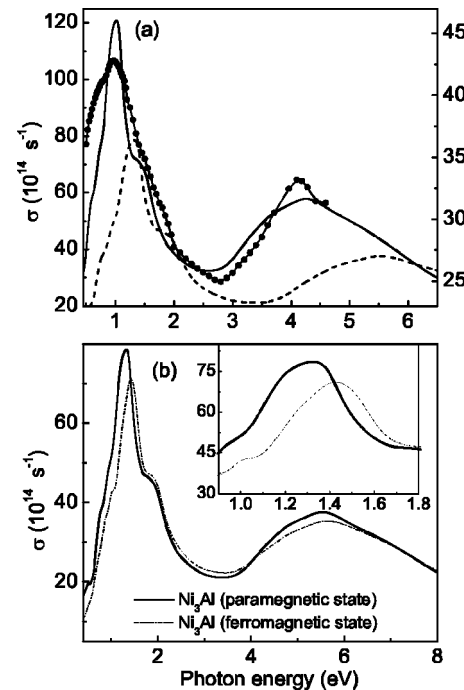


FIG. 2. (a) Experimental OC spectrum for the STOICH $\text{Ni}_{0.752}\text{Al}_{0.248}$ bulk alloy (right scale) together with theoretical ones calculated for the Ni_3Al alloy with (solid line) and without (dashed line) λ fitting after broadening. (b) Calculated OC spectra for the ferromagnetic and paramagnetic states of the stoichiometric Ni_3Al alloy. Inset shows the details of the same spectra in the near-IR region.

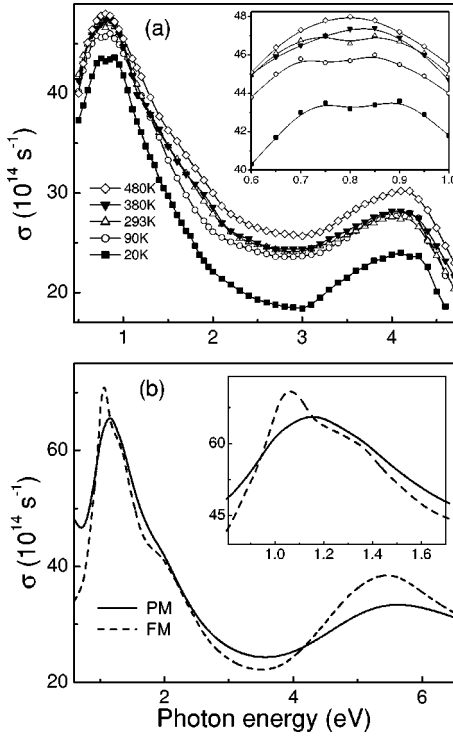


FIG. 3. (a) Experimental OC spectra for the OFF-STOICH $\text{Ni}_{0.771}\text{Al}_{0.229}$ bulk alloy measured below and above the Curie temperature. (b) Calculated OC spectra of the $\text{Ni}_{25}\text{Al}_7$ (corresponding to $\text{Ni}_{0.781}\text{Al}_{0.219}$) alloy for the ferromagnetic (FM) and paramagnetic (PM) states. Insets in both panels show the low-energy parts of these spectra in detail.

not observed earlier because of the spectral limit² or was observed as a very weak shoulder,¹ while it was theoretically predicted.^{2,4} In addition, the low-energy features of the OFF-STOICH alloy have a multiple-peak structure. The low-energy peaks in the OC spectrum for the OFF-STOICH alloy also have a double-peak structure with nearly the same intensities of both subpeaks and is slightly redshifted in comparison with the STOICH one.

The calculated OC spectrum for the paramagnetic phase of the exactly stoichiometric alloy is very similar to those in Refs. 2 and 4. The theoretical OC spectrum for the exactly stoichiometric alloy exhibits a significant resemblance in spectral shape with the experimental one for the STOICH alloy. The calculated OC spectrum also manifests a very intense interband absorption peak in the NIR region of spectra with a pronounced shoulder on its high-energy side and some feature on the low-energy slope, and also an intense absorption peak in the UV region [see Fig. 2(a)]. However, all the theoretical peaks [dashed line in Fig. 2(a)] are shifted to the high-energy side in comparison with the experimental ones. We applied the so-called λ fitting,² which partially takes into account the self-energy effects on the OC spectrum, to bring the experimental and theoretical spectral peaks into coincidence. Fig. 2(a) shows an example with $\lambda = -0.3$ determined, however, the magnitude of the calculated OC is about 2.5 times larger than the experiment. Since this fitting is not completely quantitative, we only showed that the fitted spectrum exhibits a remarkable similarity in shape to the experi-

ment. For the OFF-STOICH alloy $\lambda = -0.23$ (not shown).

The band pairs and portion of the Brillouin zone that contributed intensely to the low-energy and 4.3-eV peaks are discussed in detail elsewhere.^{2,26} Hence, in this paper we concentrate on the effects of spin polarization and slight off-stoichiometry, especially for the low-energy fine-peak structure (at ~ 1 eV). As can be seen in Figs. 2 and 3, the ferromagnetic \rightarrow paramagnetic transition in the Ni_3Al alloy affects the high-energy peak of the calculated OC spectra rather insignificantly, while there is an appreciable change for the low-energy peaks, making the details of the multiple-peak structure less pronounced and the peaks as a whole redshifted. In addition, the Ni enrichment affects the position of the low-energy peak slightly, shifting it to the low-energy side.

As discussed in Refs. 2 and 26, the bands involved in the dominating contribution to the high-energy peak are located far from the Fermi level (E_F). Since the exchange splitting of the Ni_3Al alloy is small, the majority and minority bands are shifted almost rigidly relative to the paramagnetic bands, and the amount of splitting due to the magnetic ordering is small. Therefore, the energy difference between two majority bands is nearly the same as that between two minority bands and thus the energy locations of structures in the OC spectrum do not change substantially upon the magnetic transition, resulting in very little temperature dependence [see Fig. 3(a)]. On the contrary, the initial (\mathbf{k} points near the M point, from band 9) states involved in the low-energy optical transitions are located very close to E_F , therefore, this peak may be sensitive to the magnetic transition and/or the temperature change, and we observed a rather strong temperature dependence (see Fig. 3).

In the inset of Fig. 3(b) an expanded view of the low-energy peak is presented and we can clearly see the development of a fine-peak structure of $\text{Ni}_{25}\text{Al}_7$ upon the ferromagnetic transition. A strong enhancement of the calculated OC upon the transition is observed near 1.1 eV for the off-stoichiometric $\text{Ni}_{25}\text{Al}_7$ alloy. Furthermore, the calculated peak position (~ 1.1 eV) is closer to the experimental one (~ 0.8 eV) with respect to the case of the stoichiometric Ni_3Al alloy (1.3–1.5 eV).

If the double-peak structure of the 0.8-eV feature is really due to the band splitting upon the ferromagnetic transition, the energy difference between the two subpeaks should depend on temperature. Indeed, the temperature evolution of the 0.8-eV feature can be more clearly seen in Fig. 4. We fit the OC spectra to the Lorentzian-oscillator model³² by using

$$\sigma(\omega) \equiv \frac{\omega \varepsilon_2(\omega)}{4\pi} = \frac{ne^2}{m^*} \sum_{i=0}^{i_{\max}} \frac{f_i \omega^2 \Gamma_i}{(\omega^2 - \omega_i^2)^2 + \omega^2 \Gamma_i^2}, \quad (1)$$

where n is the concentration of the conduction electrons; m^* is the effective mass of conduction electrons; and ω_i , f_i , and $1/\Gamma_i$ are the frequency, the oscillator strength, and the lifetime, respectively, of the i th oscillator. We put $i_{\max} = 6$. When $i = 0$, Eq. (1) represents the contribution of intraband transitions and $\omega_0 = 0$. As displayed in the inset of Fig. 4, the energy difference between the two subpeaks of the 0.8-eV

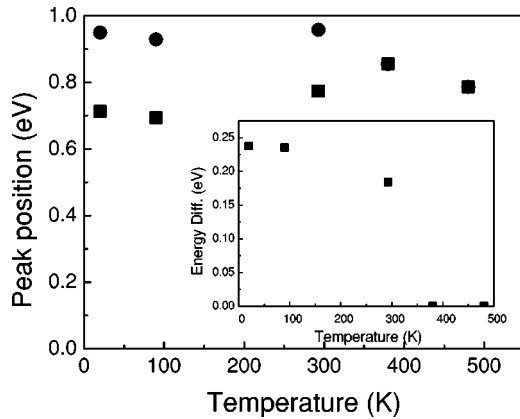


FIG. 4. Temperature evolution of the 0.8-eV double-peak structure of the OC spectra. The inset also shows the temperature evolution of the energy difference between two subpeaks.

feature is zero above 293 K. It starts to grow rapidly just below 293 K and saturates eventually as the temperature approaches 0 K.

As shown in Fig. 5, the calculated spin-resolved OC spectra for the stoichiometric Ni_3Al alloy have similar shapes to each other and have a peak at ~ 1.4 eV. Those of the off-stoichiometric $\text{Ni}_{25}\text{Al}_7$ alloy, however, show a strong enhancement of OC near 1.1 eV, which results mostly from the optical transitions between two majority bands, and thus the double-peak structure appears. It implies that the experimental double-peak structure centered at 0.8 eV and its temperature dependence shown in Fig. 3(a) are genuinely caused by the appearance of the antistructure $\text{Ni}^{(\text{Al})}$ atoms (the Ni atoms at the Al sites) in the OFF-STOICH alloy. In addition, the spin polarization is also important. Thus, according to the results of calculations one can conclude that the multiple-peak structure of the low-energy peak should disappear in the paramagnetic state of the alloy, and the observed behavior of the OFF-STOICH alloy confirms this. From the OC spectra of the OFF-STOICH alloy presented in Fig. 3 we can clearly see that the double-peak structure really disappears in the paramagnetic state. The complete disappearance of the double-peak structure, however, occurs at a temperature near RT.

A similar behavior was observed in the EKE measurements. Figure 6 presents the EKE spectrum of the OFF-

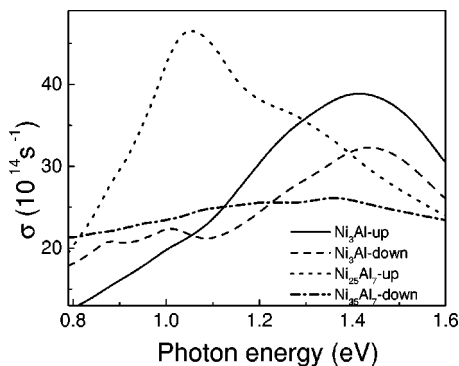


FIG. 5. Spin-resolved OC spectra of Ni_3Al and $\text{Ni}_{25}\text{Al}_7$ alloys in the ferromagnetic phase. An energy-dependent Lorentzian broadening is included.

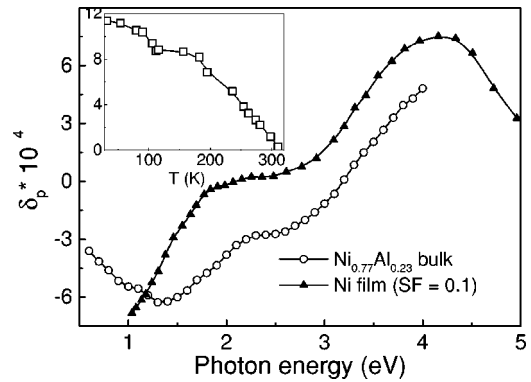


FIG. 6. EKE spectra for the bulk $\text{Ni}_{0.771}\text{Al}_{0.229}$ alloy (measured at $T=27$ K and $\varphi=77^\circ$) and for a thin Ni film (measured at $T=293$ K and $\varphi=75^\circ$: the magnitude is reduced by 0.2). Inset shows the temperature dependence of the EKE for the bulk $\text{Ni}_{0.771}\text{Al}_{0.229}$ alloy at $\hbar\omega=4$ eV and $\varphi=70^\circ$. Solid lines are only for a guide to the eyes. Note that all three measurements have different temperatures and angles of incidence.

STOICH alloy measured at $T=27$ K and an incidence angle (φ) of 77° , together with that of a Ni thin film measured at $T=293$ K and $\varphi=75^\circ$. The shape of the EKE spectrum of the OFF-STOICH alloy shows a resemblance to that of the Ni thin film, although the intensity is substantially reduced and the spectrum for the alloy is shifted by about 0.5 eV to the high-energy side. The most striking results of the EKE is its temperature dependence. The inset of Fig. 6 exhibits the temperature variation of the EKE measured at $\hbar\omega=4$ eV. The EKE signal persists up to ~ 300 K. This result is consistent with the OC measurements in which a double-peak structure centered at 0.8 eV does not disappear, at least, up to 293 K. There is a dip observed around 100 K, shown in the inset of Fig. 6.

Since the peculiar properties discussed above should be closely related to the magnetic properties of the investigated alloys, we have also measured the ac magnetic susceptibility. The Curie temperature, T_C , of the STOICH alloy was determined from an extremum of $d\chi/dT$ curves; $T_C=50.2$ K (not shown). Unlike the STOICH alloy, $\chi(T)$ of the OFF-STOICH alloy exhibits not only a low-temperature transition at $T_{C1}=87.5$ K but a high-temperature one at $T_{C2}\approx 250$ K (see Fig. 7). The obtained low-temperature values for both samples are in an excellent agreement with other measurements.^{11,33}

There are two possible explanations for the existence of T_{C2} for the OFF-STOICH alloy. It is well known that the Ni_3Al alloy is a typical weakly itinerant ferromagnet in which spin fluctuations play an important role.¹⁵ Such ferromagnets are characterized by the existence of the ferromagnetically ordered regions far above T_C . Thus, the high-temperature kink can be caused by the transition of the OFF-STOICH alloy into a true paramagnetic state. We also measured $\chi(T)$ for a single-crystal Ni_3Al alloy (not shown), however, no high-temperature transition was observed. In addition to that, according to Ref. 18, there is a crossover from spin fluctuator to ferromagnet at 75.1 at. % of Ni as the Ni concentration increases. Therefore, we can safely conclude that the spin

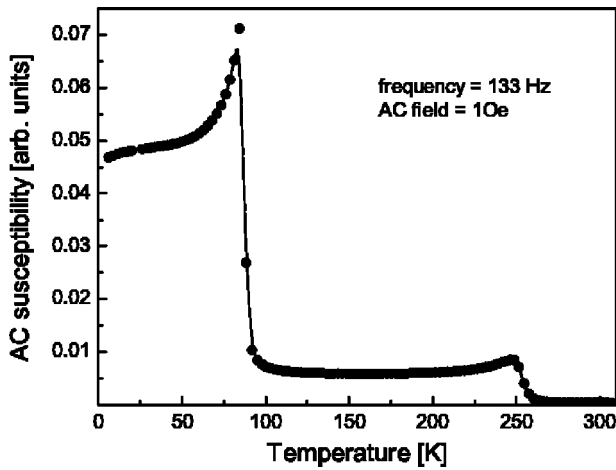


FIG. 7. Temperature dependence of the ac magnetic susceptibility for the bulk off-stoichiometric $\text{Ni}_{0.771}\text{Al}_{0.229}$ alloy.

fluctuation is unlikely the explanation for the existence of the high-temperature transition, as well as the low-temperature one.

According to another but more probable scenario, the high-temperature peculiarity in $\chi(T)$ could be associated with the presence of another ferromagnetic phase in the OFF-STOICH alloy. The phase diagram of the Ni-Al binary-alloy system reveals that at between 76 and 92 at. % of Ni at RT the alloy consists of a mixture of γ' and γ phases. The γ phase is a solid solution of Ni and Al whose T_C decreases almost linearly from 631 K for pure Ni to 363 K for the Al-rich border of the γ phase.³⁴ Therefore, the second ferromagnetic phase should have a T_{C2} significantly higher than T_{C1} as shown in Fig. 7. Furthermore, the concentration of the γ phase in the OFF-STOICH alloy should be inversely proportional to the distance from the border of the γ phase. In our case the content of the γ phase can be estimated for the OFF-STOICH alloy to be 6%. Although this concentration could be large enough to be recognized by the XRD measurements, it was not observed, probably because the γ phase has the same fcc-based crystal structure as the γ' phase with a slightly different lattice constant, resulting in only a slight asymmetry of the XRD peaks for the γ' phase. This second phase can be modeled as the appearance of antistructure Ni atoms at the Al sites, which plays a role in magnetic inhomogeneity and/or the appearance of clusters.

There are, at least, two references that explicitly reject the possibility of the presence of magnetic inhomogeneity in the Ni_3Al sample: Refs. 22 and 23. In Ref. 22 the sample was almost stoichiometric and a single crystal, therefore, the situation would be quite different from our case in which a slightly Ni-rich (~ 77 at. %) polycrystalline sample was used. In Ref. 23 the authors concluded that there was no indication of magnetic inhomogeneity in their slightly Ni-rich (75.9 at. %) single-crystalline sample by analyzing the polarized-neutron-diffraction data. Two comments can be addressed regarding conclusion. First, in their analysis they used a nominal concentration which would certainly be different from the real concentration because of the preferential evaporation of Al during arc melting.¹⁸ Therefore, the de-

duced moment of the antistructure $\text{Ni}^{(\text{Al})}$ atoms should be different since they employed the nominal concentration to obtain the magnetic moment of the $\text{Ni}^{(\text{Al})}$ atoms. Second, they concluded that the deduced magnetic moment of the $\text{Ni}^{(\text{Al})}$ atoms is not significantly different from that of the Ni atoms at the Ni sites [$\text{Ni}^{(\text{Ni})}$]. If this is true, then it is not possible to explain the strong concentration dependence of the magnetic moment of $\text{Ni}_x\text{Al}_{1-x}$ alloys; $M \propto (x - x_c)^{1/2}$. For the stoichiometric sample ($x=0.75$) the magnetic moment of Ni atoms is known to be $\sim 0.077\mu_B/\text{Ni}$.^{6,7,10-12} If there is no distinction between the magnetic moments of the $\text{Ni}^{(\text{Ni})}$ atoms and of the $\text{Ni}^{(\text{Al})}$ atoms, there is no reason to believe that the magnetic moment of the $\text{Ni}^{(\text{Ni})}$ atoms in a slightly Ni-rich sample, for example, $x=0.7641$, is different from $0.077\mu_B/\text{Ni}$. The average magnetic moment of the sample with $x=0.7641$ is $\sim 0.114\mu_B/\text{Ni}$,¹⁸ and, if we assume that the magnetic moment of the $\text{Ni}^{(\text{Ni})}$ atom is $\sim 0.077\mu_B/\text{Ni}$, that of the $\text{Ni}^{(\text{Al})}$ atom should be $2.08\mu_B/\text{Ni}$. The results of our first-principles calculations show that both the $\text{Ni}^{(\text{Al})}$ and the $\text{Ni}^{(\text{Ni})}$ atoms of a slightly Ni-rich alloy have significantly enhanced magnetic moments relative to that of the Ni atoms of the corresponding stoichiometric alloy. The $\text{Ni}^{(\text{Al})}$ atoms exhibit an increase of about a factor of 3. Furthermore, Takahashi *et al.*,¹¹ in their investigation of the effects of Pd doping in $\text{Ni}_{77.0-x}\text{Al}_{23.0}\text{Pd}_x$ ($x=0.0, 0.4, 0.8, 1.8, 2.2, \text{ and } 3.0$), observed very little variation of the magnetic moment and T_C with the Ni concentration. They argued that the doped Pd atoms have a strong tendency to occupy the Ni sites and the expelled Ni atoms occupy the Al sites, and thus the number of $\text{Ni}^{(\text{Al})}$ atoms does not change even though the Ni concentration changes, while that of the $\text{Ni}^{(\text{Ni})}$ atoms does. The magnetic properties of the samples were mainly determined by the number of $\text{Ni}^{(\text{Al})}$ atoms. Therefore, the magnetic moment of the $\text{Ni}^{(\text{Ni})}$ atoms should be substantially smaller than that of the $\text{Ni}^{(\text{Al})}$ atoms and, at least, for the Ni-rich samples there should exist a certain degree of magnetic inhomogeneity.

The dip observed in the temperature dependence of the EKE (around 100 K) reflects disappearance of the macroscopic alignment of the magnetic moments of Ni atoms at T_{C1} in the γ' phase (see Fig. 6). As discussed in the optical measurements, the EKE signal does not vanish completely above T_{C1} , rather it survives up to RT. Between T_{C1} and T_{C2} the magnetization of a great part of the sample disappears (see Fig. 7), because the majority phase is the γ' phase, while the remnant second phase has a much higher Curie temperature, which still gives the EKE signal.

The presence of the second ferromagnetic phase can also explain the temperature dependence of a double-peak structure centered at 0.8 eV for the OFF-STOICH alloy in Fig. 3(a). The double-peak structure is due to the spin ordering of the sample and hence the exchange splitting of the bands near E_F . Between T_{C1} and T_{C2} the second phase gives this exchange splitting, resulting in persistence of the double-peak structure. It disappears, however, as temperature is raised to near or slightly above T_{C2} .

The calculated magnetic moment of the ferromagnetic phase of Ni_3Al was $\sim 0.598\mu_B/\text{f.u.}$, where f.u. denotes the

formula unit, which is ~ 2.5 times larger than the experimental value [$0.24\mu_B/\text{f.u.}$ (Refs. 6,7, and 10–12)]. Unlike the argument by Min *et al.*,²⁵ the introduction of spin-orbit interactions essentially does not alter the results. We also tried to include the generalized-gradient approximation, however, the calculated magnetic moment is even larger (about $0.7\mu_B/\text{f.u.}$). The aforementioned disorder-II case gives an average magnetic moment of $0.598\mu_B/\text{f.u.}$, while for the disorder-I case it is further reduced ($0.580\mu_B/\text{f.u.}$). The reduction of the magnetic moment due to the “disorder” is not large enough to resolve the discrepancy between experiment and calculation. We do not know at present whether the discrepancy can be attributed to the presence of additional degrees of disorder in the sample and/or the deficiency of the LSDA. One more point deserves a comment. The Ni atoms at different sites have different magnetic moments; the $\text{Ni}^{(\text{Al})}$ atom has $0.65\text{--}0.71\mu_B$ and the $\text{Ni}^{(\text{Ni})}$ atoms carry a smaller value, depending on the distance to the $\text{Ni}^{(\text{Al})}$ atom. The larger the distance to the $\text{Ni}^{(\text{Al})}$ atom, the smaller the magnetic moment. The calculated magnetic moment for the $\text{Ni}_{25}\text{Al}_7$ alloy is $1.012\mu_B/\text{f.u.}$

These two types of supercell calculations can lead us to the following conclusions. (i) The calculated magnetic moment of the stoichiometric Ni_3Al alloy is significantly larger than that of the experiments, and a slight disordering or the interchange between the Ni and Al atoms may reduce the average magnetic moment, but not significantly. (ii) The antistructure $\text{Ni}^{(\text{Al})}$ atoms carry a large moment and they are magnetically different from the neighboring $\text{Ni}^{(\text{Ni})}$ atoms. There is, therefore, a possibility of the presence of magnetic inhomogeneity for a slightly Ni-rich off-stoichiometric Ni_3Al alloy. Our investigations on the optical and MO properties also confirm this argument.

V. SUMMARY

Optical, MO, and magnetic properties of nearly stoichiometric ($\text{Ni}_{0.752}\text{Al}_{0.248}$) and slightly off-stoichiometric ($\text{Ni}_{0.771}\text{Al}_{0.229}$) alloys have been experimentally studied in a

wide temperature range. The OC spectra of both alloys exhibit intense multiple peaks in the NIR region of the spectra, whose existence was predicted earlier by theory but not confirmed by experiments. The multiple-peak structure in the NIR region as well as the MO response for $\text{Ni}_{0.771}\text{Al}_{0.229}$ persist up to RT. These temperature dependencies of the optical and MO properties of the alloy can be attributed to the presence of a magnetic inhomogeneity and/or clusters in the sample between $T_{C1} \approx 87.5$ K and $T_{C2} \approx 250$ K. The results of ac susceptibility measurements support this argument.

The influence of spin ordering (paramagnetic-to-ferromagnetic transition) and Ni enrichment on the optical properties of Ni_3Al alloys have been investigated theoretically and experimentally. It was shown that the multiple-peak structure of the low-energy peaks for both investigated alloys originates from the appearance of the antistructure Ni atoms at the Al sites. It was also theoretically shown that a slight atomic disorder leads to a decrease of the magnetic moment for the stoichiometric Ni_3Al alloy and that a deviation from the equiatomic composition to the Ni-rich side causes an enhancement of the total magnetic moment. For the case of the $\text{Ni}_{25}\text{Al}_7$ alloy, the magnetic moment is dominated by the antistructure Ni atoms at the Al sites.

It is certainly very important to know more about the relative structures of the two samples experimentally using, for instance, x-ray-absorption fine-structure spectroscopy, and especially about the spatial distribution of defects in the off-stoichiometry sample. This work will be done in the near future.

ACKNOWLEDGMENTS

We would like to acknowledge E. A. Gañshina for the MO measurements, as well as B. Idzikowski for the help in the magnetic and structural measurements. This work was supported by the KOSEF through Quantum Photonic Science Research Center at Hanyang University and by Korea Research Foundation (Grant Nos. KRF-01-015-DS0015 and KRF-01-DP0193).

*Electronic address: rheejy@office.hoseo.ac.kr

†Electronic address: yplee@hanyang.ac.kr

¹P.A.M. van der Heide, J.J.M. Buiting, L.M. ten Dam, L.W.M. Schreurs, R.A. de Groot, and A.R. de Vroomen, *J. Phys. F: Met. Phys.* **15**, 1195 (1985).

²J.Y. Rhee, B.N. Harmon, and D.W. Lynch, *Phys. Rev. B* **55**, 4124 (1997).

³J.J.M. Buiting, J. Kübler, and F.M. Mueller, *J. Phys. F: Met. Phys.* **13**, L179 (1983).

⁴M.A. Khan, A. Kashyap, A.K. Solanki, T. Nautiyal, and S. Auluck, *Phys. Rev. B* **48**, 16 974 (1993).

⁵G.P. Pells and M. Shiga, *J. Phys. C* **2**, 1835 (1969).

⁶F.R. de Boer, C.J. Schinkel, J. Biesterbos, and S. Proost, *J. Appl. Phys.* **40**, 1049 (1969).

⁷T.F.M. Kortekaas and J.J.M. Franse, *J. Phys. F: Met. Phys.* **6**, 1161 (1976).

⁸J.J.M. Franse, *Physica B & C* **86-88**, 283 (1977).

⁹N. Buis, J.J.M. Franse, and P.E. Brommer, *Physica B & C* **106**, 1

(1981).

¹⁰H. Sasakura, K. Suzuki, and Y. Masuda, *J. Phys. Soc. Jpn.* **53**, 352 (1984); **53**, 754 (1984).

¹¹S. Takahashi, A.Y. Takahashi, and A. Chiba, *J. Phys.: Condens. Matter* **6**, 6011 (1994).

¹²A. Semwal and S.N. Kaul, *Phys. Rev. B* **60**, 12 799 (1999).

¹³E.C. Stoner, *Proc. R. Soc. London, Ser. A* **139**, 339 (1939); D.M. Edwards and E.P. Wohlfarth, *ibid.* **303**, 127 (1968); E.P. Wohlfarth, *Rev. Mod. Phys.* **25**, 211 (1953).

¹⁴T. Moriya and A. Kawabata, *J. Phys. Soc. Jpn.* **34**, 639 (1973); **35**, 669 (1973).

¹⁵S.N. Kaul and A. Semwal, *Phys. Lett. A* **254**, 101 (1999); S.N. Kaul, *J. Phys.: Condens. Matter* **11**, 7597 (1994).

¹⁶N.R. Bernhoeft, I. Cole, G.G. Lonzarich, and G.L. Squires, *J. Appl. Phys.* **53**, 8024 (1982).

¹⁷N.R. Bernhoeft, G.G. Lonzarich, P.W. Mitchell, and D.M. Paul, *Phys. Rev. B* **28**, 422 (1983).

¹⁸S.K. Dhar and K.A. Gschneidner, Jr., *Phys. Rev. B* **39**, 7453

- (1989); S.K. Dhar, K.A. Gschneidner, Jr., L.L. Miller, and D.C. Johnston, *ibid.* **40**, 11 488 (1989).
- ¹⁹C.G. Robbins and H. Claus, AIP Conf. Proc. **5**, 527 (1971).
- ²⁰A. Parthasarathi and P.A. Beck, AIP Conf. Proc. **29**, 282 (1975).
- ²¹W. de Dood and P.F. de Chatel, J. Phys. F: Met. Phys. **3**, 1039 (1973).
- ²²C. Stassis, F.X. Kayser, C.-K. Loong, and D. Arch, Phys. Rev. B **24**, 3048 (1981).
- ²³G.P. Felcher, J.S. Kouvel, and A.E. Miller, Phys. Rev. B **16**, 2124 (1977).
- ²⁴D. Hackenbracht and J. Kübler, J. Phys. F: Met. Phys. **10**, 427 (1980).
- ²⁵B.I. Min, A.J. Freeman, and H.J.F. Jansen, Phys. Rev. B **37**, 6757 (1988).
- ²⁶J.Y. Rhee, Yu.V. Kudryavtsev, K.W. Kim, and Y.P. Lee, J. Korean Phys. Soc. **36**, 404 (2000).
- ²⁷We used the computer code TB-LMTO-ASA program, version 47, developed by Professor Andersen's group. See O.K. Andersen, Phys. Rev. B **12**, 3060 (1975); O.K. Andersen and O. Jepsen, Phys. Rev. Lett. **53**, 2571 (1984).
- ²⁸L. Hedin and B.I. Lundqvist, J. Phys. C **4**, 2064 (1971).
- ²⁹U. von Barth and L. Hedin, J. Phys. C **5**, 1629 (1972).
- ³⁰Y.M. Gu and L. Fritsche, J. Phys.: Condens. Matter **4**, 1905 (1992).
- ³¹J.Y. Rhee, J. Korean Phys. Soc. **34**, 191 (1999).
- ³²F. Wooten, *Optical Properties of Solids* (Academic, New York, 1972), p. 45.
- ³³M. Yoshizawa, H. Seki, K. Ikeda, K. Okuno, M. Saito, and K. Shigematsu, J. Phys. Soc. Jpn. **61**, 3313 (1992).
- ³⁴R. M. Bozorth, *Ferromagnetism* (IEEE, New York, 1993), p. 300.